PERGAMON

International Journal of Solids and Structures 38 (2001) 1903–1918

INTERNATIONAL JOURNAL OF SOLIDS and STRUCTURES

www.elsevier.com/locate/ijsolstr

Analysis of indentation cracking in piezoceramics

L.Z. Jiang, C.T. Sun *

School of Aeronautics and Astronautics, Grissom Hall 325, Purdue University, West Lafayette, IN 47907-1282, USA

Received 16 August 1999; in revised form 6 March 2000

Abstract

The electric field can significantly affect the growth of Vickers indentation cracks in piezoceramics. In this study, the wedge effect caused by inelastic deformation was proposed to explain the phenomenon. An approximate analytic solution for a half penny-shaped crack in a piezoceramic half space was derived from modifying full penny-shaped crack solution according to proper boundary conditions on the free surface of the indented piezoceramic specimen. The solution in conjunction with the mechanical strain energy release rate was used to quantitatively account for the effect of electric field on crack length produced by Vickers indentations with various indentation forces. The proposed model was able to explain the effects of electric field on crack growth in piezoceramics. © 2001 Elsevier Science Ltd. All rights reserved.

Keywords: Indentation cracking; Piezoceramics; Electric field; Mechanical strain energy release rate; Domain switching

1. Introduction

Piezoceramics are commonly used for actuators. They are very brittle and are susceptible to fracture. In operation, piezoceramic actuators are subjected to both mechanical and electrical loads. Recently, the behavior of cracks and fracture toughness in piezoceramics under combined mechanical and electrical loads had been a subject of research interest (Deeg, 1980; McMeeking, 1990; Pak, 1990; Sosa and Pak, 1990; Sosa, 1992; Suo et al., 1992; Park and Sun, 1995a,b).

The indentation technique has been used to characterize material properties and fracture toughness of brittle materials (Chiang et al., 1982; Tsai, 1984; Cook and Pharr, 1990; Anstis et al., 1981) because it is simple and can be performed on small specimens. Sridhar et al. (1999) employed the indentation technique to characterize piezoelectric material properties using different electric boundary conditions for the indenter. Giannakopoulos and Suresh (1999) developed a theory for axisymmetric indentation of piezoelectric materials based on which the experimental results by Ramamurty et al. (1999) were explained. Chen et al. (1999) analyzed the elasto-electric field for a rigid conical punch on a transversely isotropic piezoelectric

* Corresponding author. Tel.: +1-765-494-5130; fax: +1-765-494-0307.
E-mail address: sun@ecn.purdue.edu (C.T. Sun).

0020-7683/01/$ - see front matter
PII: S0020-7683(00)00142-6

half space. Many researchers (Okazaki, 1984; Tobin and Pak, 1993; Cao and Evans, 1995; Sun and Park, 1995) have employed the Vickers indentation technique to characterize fracture toughness for piezoceramics. It has been observed that the electric field has a significant effect on the apparent toughness of piezoceramics. Specifically, a positive electric field (in the poling direction) decreases the apparent toughness while a negative electric field increases the apparent toughness. This trend is identical to the results by Park and Sun (1995b) using the compact tension specimen. Park and Sun (1995b) proposed the use of the mechanical strain energy release rate as a measure of fracture toughness and were able to account for the effect of electric field on fracture toughness. Jiang and Sun (1999) employed the fracture parameter to successfully characterize the fatigue behavior of piezoceramics.

The crack growth mechanism for a crack produced by the Vickers indentation is quite different from that in the conventional fracture test with compact tension specimens. For Vickers indentation, inelastic deformation under the indenter would give rise to tensile opening stress at the crack front (Yoffe, 1982). These tensile stresses would propagate the crack to its final dimension. To employ the mechanical strain energy release rate to predict the growth of a Vickers indentation induced crack in the presence of electric fields, these crack front residual stresses must be determined.

It is known that a half penny-shaped crack is formed after indentation in some brittle materials (Chandrasekar and Chaudhri, 1993) and in piezoceramics (Sun and Park, 1995). Fig. 1 shows the surface view of the cracks produced by Vickers indentation and the half penny-shaped crack beneath the surface in PZT-4. It is noted that the crack front forms a perfect half circle. No crack bridging was observed.

Before presenting the solution for a half penny-shaped crack embedded in piezoelectric media, a review of relevant literature is appropriate. Wang (1992) investigated a flat elliptical crack in a piezoelectric material by utilizing the eigenstrain approach. His solution involves the evaluation of residue of generalized integrals but no explicit results are available. Wang and Huang (1995) studied an elliptical crack in transversely isotropic media under a very specific loading condition, i.e., uniform pressure and uniform charge on the insulated crack surface using the potential function approach. It is noted from their solution that the stress intensity factor depends not only on the applied uniform pressure, but on the uniform charge as well, while the electric displacement intensity factor depends on both charge and pressure. This appears inconsistent with the existing two-dimensional (Pak, 1990, 1992; Sosa, 1992; Suo et al., 1992) and three-dimensional (Sosa and Pak, 1990) solutions. In addition, their solution cannot be used to obtain the solution for point force and point charge applied on the crack surface that is essential to the Vickers indentation problem. Huang (1997) considered a similar problem as Wang (1992) using an eigenstrain formulation and Cauchy's residue theorem, but no closed form solution was reported. Kogan et al. (1996) considered the conductive boundary condition and obtained the stress intensity factor and near tip solution. However, in the experimental results conducted by Sun and Park (1995), Vickers indented specimen was immersed in silicon oil and the crack surface was covered by oil. Due to the several orders of magnitude difference between the values of the dielectric constants of silicon oil and PZT, it is believed that the impermeable crack surface boundary condition is a good description of the testing condition.

In this study, the electro-elastic solution for a penny-shaped crack under arbitrarily axisymmetric loading conditions was obtained by using the Hankel transform and solving dual integral equations. The point load solution was easily obtained from the general solution by taking limiting process. The effect of the inelastic deformation was represented by a double force applied at the center of the penny-shaped crack. For a half penny-shaped crack, a correction factor was added to account for the free surface condition of the half space. Such an approach was employed by Smith et al. (1967a,b) and Kassir and Sih (1968) for a similar problem in elastic solids. The approximation was then used to calculate the mechanical strain energy release rate to predict Vickers indentation induced crack lengths for different indentation loads and electric fields.

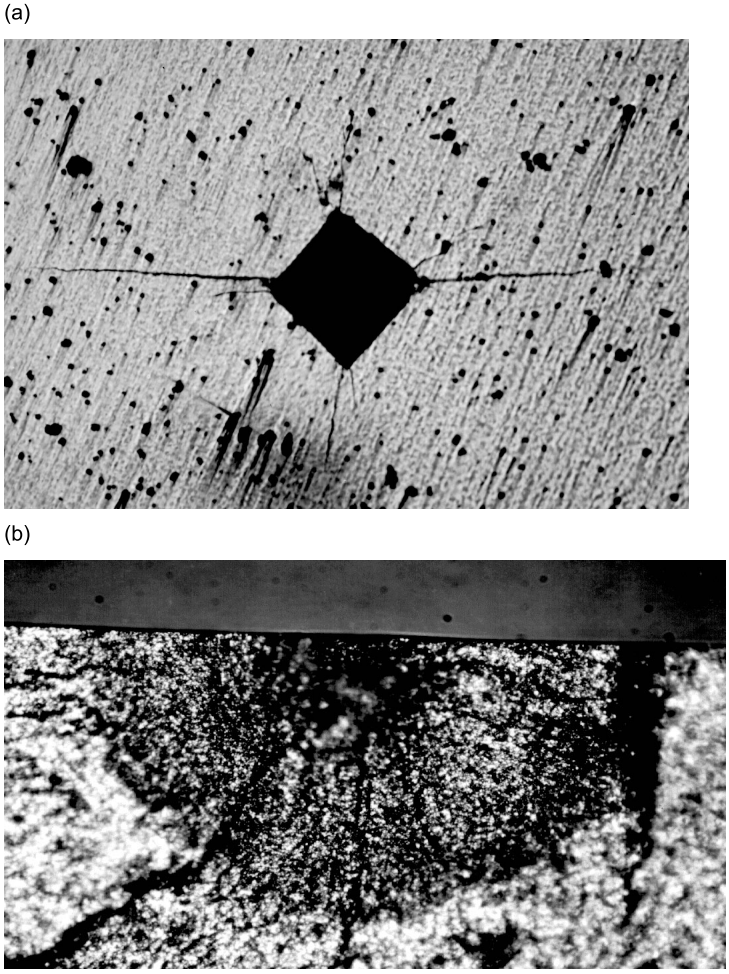

Fig. 1. (a) Vickers indentation induced crack (Sun and Park, 1995) and (b) typical indentation induced crack beneath the surface (Sun and Park, 1995).

2. Axisymmetric piezoelectric body

In the absence of body forces, the equilibrium equations for an axisymmetric piezoelectric body under axisymmetric loading can be expressed as

$$\begin{aligned} &\frac{\partial \sigma_{rr}}{\partial r}+\frac{\partial \tau_{rz}}{\partial z}+\frac{\sigma_{rr}-\sigma_{\theta\theta}}{r}=0,\\ &\frac{\partial \tau_{rz}}{\partial r}+\frac{\partial \sigma_{zz}}{\partial z}+\frac{\tau_{rz}}{r}=0, \end{aligned} \tag{1}$$

and the Gauss law is

$$\frac{\partial}{\partial r}(rD_r)+r\frac{\partial}{\partial z}(D_z)=0, \tag{2}$$

where σ, τ and D are the normal stress, shear stress, and electric displacement, respectively, and r, θ and z are the radial, circumferential and axial coordinates, respectively.

Assume that the z-direction is parallel to the poling direction. Most man-made piezoelectric materials are transversely isotropic and possess the following constitutive relations (Tiersten, 1969):

$$\begin{Bmatrix} \sigma_{rr} \\ \sigma_{\theta\theta} \\ \sigma_{zz} \\ \tau_{rz} \end{Bmatrix} = \begin{bmatrix} c_{11} & c_{12} & c_{13} & 0 \\ c_{12} & c_{11} & c_{13} & 0 \\ c_{13} & c_{13} & c_{33} & 0 \\ 0 & 0 & 0 & c_{44} \end{bmatrix} \begin{Bmatrix} \gamma_{rr} \\ \gamma_{\theta\theta} \\ \gamma_{zz} \\ \gamma_{rz} \end{Bmatrix} - \begin{bmatrix} 0 & e_{31} \\ 0 & e_{31} \\ 0 & e_{33} \\ e_{15} & 0 \end{bmatrix} \begin{Bmatrix} E_r \\ E_z \end{Bmatrix}, \tag{3}$$

$$\begin{Bmatrix} D_r \\ D_z \end{Bmatrix} = \begin{bmatrix} 0 & 0 & 0 & e_{15} \\ e_{31} & e_{31} & e_{33} & 0 \end{bmatrix} \begin{Bmatrix} \gamma_{rr} \\ \gamma_{\theta\theta} \\ \gamma_{zz} \\ \gamma_{rz} \end{Bmatrix} + \begin{bmatrix} \varepsilon_{11} & 0 \\ 0 & \varepsilon_{33} \end{bmatrix} \begin{Bmatrix} E_r \\ E_z \end{Bmatrix}, \tag{4}$$

where c_{ij}, e_{ij} and ε_{ij} are elastic, piezoelectric and dielectric constants, respectively, and strains and electric fields are given by

$$\begin{aligned} &\gamma_{rr} = \frac{\partial u}{\partial r}, \quad \gamma_{\theta\theta} = \frac{u}{r}, \quad \gamma_{zz} = \frac{\partial w}{\partial z}, \quad \gamma_{rz} = \frac{\partial u}{\partial z} + \frac{\partial w}{\partial r}, \\ &E_r = -\frac{\partial \phi}{\partial r} \quad \text{and} \quad E_z = -\frac{\partial \phi}{\partial z}, \end{aligned} \tag{5}$$

in which u and w are displacements in r and z directions, respectively, and ϕ is electric potential.

Eliminating stresses and electric displacements from Eqs. (1) and (2) using Eqs. (3)–(5) leads to

$$\begin{aligned} &c_{11}\left(\frac{\partial^2 u}{\partial r^2} + \frac{1}{r}\frac{\partial u}{\partial r} - \frac{u}{r^2}\right) + c_{44}\frac{\partial^2 u}{\partial z^2} + (c_{13} + c_{44})\frac{\partial^2 w}{\partial r \partial z} + (e_{15} + e_{31})\frac{\partial^2 \phi}{\partial r \partial z} = 0, \\ &(c_{13} + c_{44})\frac{\partial}{r\partial r}\left(r\frac{\partial u}{\partial z}\right) + c_{44}\left(\frac{\partial^2 w}{\partial r^2} + \frac{1}{r}\frac{\partial w}{\partial r}\right) + c_{33}\frac{\partial^2 w}{\partial z^2} + e_{15}\left(\frac{\partial^2 \phi}{\partial r^2} + \frac{1}{r}\frac{\partial \phi}{\partial r}\right) + e_{33}\frac{\partial^2 \phi}{\partial z^2} = 0, \\ &(e_{15} + e_{31})\frac{\partial}{r\partial r}\left(r\frac{\partial u}{\partial z}\right) + e_{15}\left(\frac{\partial^2 w}{\partial r^2} + \frac{1}{r}\frac{\partial w}{\partial r}\right) + e_{33}\frac{\partial^2 w}{\partial z^2} - \varepsilon_{11}\left(\frac{\partial^2 \phi}{\partial r^2} + \frac{1}{r}\frac{\partial \phi}{\partial r}\right) - \varepsilon_{33}\frac{\partial^2 \phi}{\partial z^2} = 0. \end{aligned} \tag{6}$$

The Hankel transform pair is defined by

$$\left.\begin{aligned} \overline{F}(\xi, z) &= \int_0^\infty F(r, z) r J_k(\xi r)\, \mathrm{d}r, \\ F(r, z) &= \int_0^\infty \overline{F}(\xi, z) \xi J_k(\xi r)\, \mathrm{d}\xi, \end{aligned}\right| \tag{7}$$

where J_k is Bessel's function of the first kind of order k. Applying the Hankel transform to Eq. (6) with $k = 1$ for u, and $k = 0$ for w and ϕ, we obtain

$$\begin{aligned} &c_{44}\overline{u}'' - c_{11}\xi^2\overline{u} - \xi(c_{13} + c_{44})\overline{w}' - \xi(e_{15} + e_{31})\overline{\phi}' = 0, \\ &(c_{13} + c_{44})\xi\overline{u}' + c_{33}\overline{w}'' - c_{44}\xi^2\overline{w} + e_{33}\overline{\phi}'' - \xi^2 e_{15}\overline{\phi} = 0, \\ &(e_{15} + e_{31})\xi\overline{u}' + e_{33}\overline{w}'' - e_{15}\xi^2\overline{w} - \varepsilon_{33}\overline{\phi}'' + \varepsilon_{11}\xi^2\overline{\phi} = 0 \end{aligned} \tag{8}$$

in which a prime indicates the derivative with respect to z. It is known that when $z \to \infty$, $\overline{u}$, $\overline{w}$ and $\overline{\phi}$ decay to zero. Following Sneddon and Lowengrub (1968), Shindo et al. (1990), and Lee and Jiang (1994), we assume the solution

$$\begin{aligned}\overline{u}(\xi,z) &= \hat{u}(\xi)\mathrm{e}^{-\eta\xi z},\\ \overline{w}(\xi,z) &= \hat{w}(\xi)\mathrm{e}^{-\eta\xi z},\\ \overline{\phi}(\xi,z) &= \hat{\phi}(\xi)\mathrm{e}^{-\eta\xi z}.\end{aligned} \tag{9}$$

Substituting the above equations into Eq. (8) and considering non-trivial solutions for $\hat{U}$, $\hat{W}$ and $\hat{\phi}$, we obtain the characteristic equation in η

$$\eta^6 + B_1\eta^4 + B_2\eta^2 + B_3 = 0, \tag{10}$$

where

$$\begin{aligned}B_1 &= \frac{e_{33}C_1 + \varepsilon_{33}C_2 + c_{33}C_3}{c_{44}(c_{33}\varepsilon_{33} + e_{33}^2)},\\ B_2 &= \frac{c_{11}C_4 + c_{44}C_5 + c_{13}C_6}{c_{44}(c_{33}\varepsilon_{33} + e_{33}^2)},\\ B_3 &= -\frac{c_{11}(c_{44}\varepsilon_{11} + e_{15}^2)}{c_{44}(c_{33}\varepsilon_{33} + e_{33}^2)},\\ C_1 &= -c_{11}e_{33} + 2c_{13}e_{15} + 2e_{31}c_{13} + 2e_{31}c_{44},\\ C_2 &= c_{13}^2 + 2c_{13}c_{44} - c_{11}c_{33},\\ C_3 &= -(e_{15} + e_{31})^2 - \varepsilon_{11}c_{44},\\ C_4 &= 2e_{15}e_{33} + \varepsilon_{11}c_{33} + c_{44}\varepsilon_{33},\\ C_5 &= e_{31}^2 - 2\varepsilon_{11}c_{13},\\ C_6 &= -\varepsilon_{11}c_{13} - 2e_{15}^2 - 2e_{15}e_{31}.\end{aligned} \tag{11}$$

Since these coefficients are real, the above bi-cubic equation, in general, has six roots, say ($\pm\eta_1$, $\pm\eta_2$ and $\pm\eta_3$), where η_1 is a real number and η_2 and η_3 are, in general, a pair of complex conjugates. Without loss of generality, we assume that η_1 and the real parts of η_2 and η_3 are positive. For the upper half space ($z \geqslant 0$), we take the solutions associated with η_1, η_2, η_3 and the corresponding characteristic functions $f_i(\xi)$ $(i = 1, 2, 3)$. Subsequently, $\hat{u}(\xi)$, $\hat{w}(\xi)$, and $\hat{\phi}(\xi)$ are expressed in terms of $f_i(\xi)$, from which the inverse transform yields

$$\begin{aligned}u(r,z) &= \sum_{i=1}^{3}\alpha_i\int_0^\infty f_i(\xi)\mathrm{e}^{-\eta_i\xi z}J_1(\xi r)\,\mathrm{d}\xi,\\ w(r,z) &= \sum_{i=1}^{3}\beta_i\int_0^\infty f_i(\xi)\mathrm{e}^{-\eta_i\xi z}J_0(\xi r)\,\mathrm{d}\xi,\\ \phi(r,z) &= \sum_{i=1}^{3}\gamma_i\int_0^\infty f_i(\xi)\mathrm{e}^{-\eta_i\xi z}J_0(\xi r)\,\mathrm{d}\xi,\end{aligned} \tag{12}$$

where

$$\begin{aligned}\alpha_i &= \frac{(e_{15} + e_{31})(c_{33}\eta_i^2 - c_{44}) - (e_{33}\eta_i^2 - e_{15})(c_{13} + c_{44})}{(c_{44}\eta_i^2 - c_{11})(e_{33}\eta_i^2 - e_{15}) + \eta_i^2(e_{15} + e_{31})(c_{13} + c_{44})},\\ \beta_i &= 1/\eta_i,\\ \gamma_i &= -[\alpha_i(c_{44}\eta_i^2 - c_{11}) + (c_{13} + c_{44})]/[(e_{15} + e_{31})\eta_i].\end{aligned} \tag{13}$$

Using Eqs. (3) and (4), we obtained stress components and electric displacement as

$$\begin{aligned}
\sigma_{zz}(r,z) &= \sum_{i=1}^{3}(c_{13}\alpha_i - c_{33}\eta_i\beta_i - e_{33}\eta_i\gamma_i)\int_0^\infty \xi f_i(\xi)\mathrm{e}^{-\eta_i\xi z}J_0(\xi r)\,\mathrm{d}\xi,\\
\tau_{rz}(r,z) &= \sum_{i=1}^{3}(-c_{44}\beta_i - c_{44}\eta_i\alpha_i - e_{15}\gamma_i)\int_0^\infty \xi f_i(\xi)\mathrm{e}^{-\eta_i\xi z}J_1(\xi r)\,\mathrm{d}\xi,\\
D_z(r,z) &= \sum_{i=1}^{3}(e_{31}\alpha_i - e_{33}\eta_i\beta_i + \varepsilon_{33}\eta_i\gamma_i)\int_0^\infty \xi f_i(\xi)\mathrm{e}^{-\eta_i\xi z}J_0(\xi r)\,\mathrm{d}\xi.
\end{aligned} \tag{14}$$

The unknown functions $f_i(\xi)$ $(i = 1, 2, 3)$ are to be determined by using boundary conditions.

3. Solution for penny-shaped crack

Consider a penny-shaped crack of radius c lying on the plane $z = 0$ in an infinite piezoelectric body (Fig. 2). The crack surfaces are subjected to an axisymmetric internal pressure $p(r)$ and charge $q(r)$. As a result of the symmetry, shear stress τ_{rz} vanishes in the plane $z = 0$. Thus, from Eq. (14),

$$\sum_{i=1}^{3}(-c_{44}\beta_i - c_{44}\eta_i\alpha_i - e_{15}\gamma_i)f_i = 0. \tag{15}$$

Using Eq. (15), f_3 can be expressed in terms of f_1 and f_2. Consequently, Eqs. (11) and (14) can be rewritten in terms of f_1 and f_2. Subsequently, the solutions at $z = 0$ are obtained as

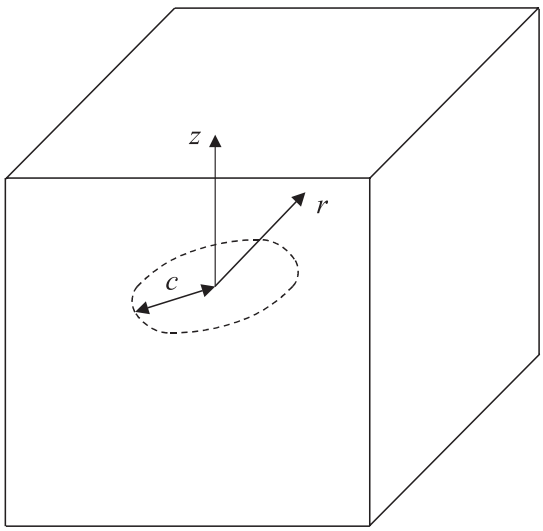

Fig. 2. Coordinates for penny-shaped crack. The poling direction is parallel to the z-axis.

$$\begin{aligned}
\sigma_{zz}(r,0) &= k_{11}\int_0^\infty f_1(\xi)\xi J_0(\xi r)\,\mathrm{d}\xi + k_{12}\int_0^\infty f_2(\xi)\xi J_0(\xi r)\,\mathrm{d}\xi,\\
D_z(r,0) &= k_{21}\int_0^\infty f_1(\xi)\xi J_0(\xi r)\,\mathrm{d}\xi + k_{22}\int_0^\infty f_2(\xi)\xi J_0(\xi r)\,\mathrm{d}\xi,\\
w(r,0) &= (\beta_1+\beta_3\Delta_1)\int_0^\infty f_1(\xi)J_0(\xi r)\,\mathrm{d}\xi + (\beta_2+\beta_3\Delta_2)\int_0^\infty f_2(\xi)J_0(\xi r)\,\mathrm{d}\xi,\\
\phi(r,0) &= (\gamma_1+\gamma_3\Delta_1)\int_0^\infty f_1(\xi)J_0(\xi r)\,\mathrm{d}\xi + (\gamma_2+\gamma_3\Delta_2)\int_0^\infty f_2(\xi)J_0(\xi r)\,\mathrm{d}\xi,
\end{aligned} \tag{16}$$

where

$$\begin{aligned}
\Delta_1 &= -\frac{c_{44}\beta_1 + c_{44}\eta_1\alpha_1 + e_{15}\gamma_1}{c_{44}\beta_3 + c_{44}\eta_3\alpha_3 + e_{15}\gamma_3},\\
\Delta_2 &= -\frac{c_{44}\beta_2 + c_{44}\eta_2\alpha_2 + e_{15}\gamma_2}{c_{44}\beta_3 + c_{44}\eta_3\alpha_3 + e_{15}\gamma_3},\\
k_{11} &= c_{13}\alpha_1 - \eta_1\beta_1 c_{33} - \gamma_1\eta_1 e_{33} + \Delta_1(c_{13}\alpha_3 - \eta_3\beta_3 c_{33} - \gamma_3\eta_3 e_{33}),\\
k_{12} &= c_{13}\alpha_2 - \eta_2\beta_2 c_{33} - \gamma_2\eta_2 e_{33} + \Delta_2(c_{13}\alpha_3 - \eta_3\beta_3 c_{33} - \gamma_3\eta_3 e_{33}),\\
k_{21} &= e_{31}\alpha_1 - \eta_1\beta_1 e_{33} + \gamma_1\eta_1\varepsilon_{33} + \Delta_1(e_{31}\alpha_3 - \eta_3\beta_3 e_{33} + \gamma_3\eta_3\varepsilon_{33}),\\
k_{22} &= e_{31}\alpha_2 - \eta_2\beta_2 e_{33} + \gamma_2\eta_2\varepsilon_{33} + \Delta_2(e_{31}\alpha_3 - \eta_3\beta_3 e_{33} + \gamma_3\eta_3\varepsilon_{33}).
\end{aligned} \tag{17}$$

Applying the crack surface and symmetry conditions at $z = 0$, i.e.,

$$\begin{aligned}
&w(r,0) = \phi(r,0) = 0 \quad \text{for } r > c,\\
&\sigma_z = -p(r) \text{ and } \quad D_z = q(r) \quad \text{for } r < c
\end{aligned} \tag{18}$$

and substituting Eq. (16) into Eq. (18), we obtain two pairs of integral equations ($i = 1$ and 2)

$$\begin{aligned}
&\int_0^\infty f_i(\varsigma)\varsigma J_0(\rho\varsigma)\,\mathrm{d}\varsigma = t_{i1}p + t_{i2}q, \quad \rho < 1,\\
&\int_0^\infty f_i(\varsigma)\varsigma J_0(\rho\varsigma)\,\mathrm{d}\varsigma = 0, \quad \rho > 1,
\end{aligned} \tag{19}$$

where $\rho = r/c$ and

$$\begin{aligned}
t_{11} &= \frac{k_{22}c^2}{k_{11}k_{22} - k_{12}k_{21}}, \qquad t_{12} = -\frac{k_{12}c^2}{k_{11}k_{22} - k_{12}k_{21}},\\
t_{21} &= -\frac{k_{21}c^2}{k_{11}k_{22} - k_{12}k_{21}}, \qquad t_{22} = \frac{k_{11}c^2}{k_{11}k_{22} - k_{12}k_{21}}.
\end{aligned} \tag{20}$$

Dual integral equations of this type have been considered by Titchmarsh (1937) and Busbridge (1938). The solution can be expressed in the form

$$f_i(\varsigma) = \frac{2}{\pi}\int_0^1 \mu\sin(\mu\varsigma)\,\mathrm{d}\mu \int_0^1 \frac{\rho(t_{i1}p(\rho) + t_{i2}q(\rho))}{\sqrt{1-\rho^2}}\,\mathrm{d}\rho. \tag{21}$$

For given $p(\rho)$ and $q(\rho)$, functions f_i can be obtained from Eq. (21). If uniform pressure p_0 and surface charge q_0 are applied over the areas of radii $a \leqslant c$ and $b \leqslant c$, respectively, the crack surface displacement, electric potential, crack tip stress, and electric displacement are obtained from Eq. (21) and then Eq. (16) as

$$w(\rho,0)=\frac{2p_0c}{\pi}\{(\beta_1+\beta_3\Delta_1)t_{11}+(\beta_2+\beta_3\Delta_2)t_{21}\}\left(1-\sqrt{1-(a/c)^2}\right)\sqrt{1-\rho^2}$$
$$+\frac{2q_0c}{\pi}\{(\beta_1+\beta_3\Delta_1)t_{12}+(\beta_2+\beta_3\Delta_2)t_{22}\}(1-\sqrt{1-(b)})\sqrt{1-\rho^2},\quad \rho\leqslant 1, \tag{22}$$

$$\phi(\rho,0)=\frac{2p_0c}{\pi}\{(\gamma_1+\gamma_3\Delta_1)t_{11}+(\gamma_2+\gamma_3\Delta_2)t_{21}\}\left(1-\sqrt{1-(a/c)^2}\right)\sqrt{1-\rho^2}$$
$$+\frac{2q_0c}{\pi}\{(\gamma_1+\gamma_3\Delta_1)t_{12}+(\gamma_2+\gamma_3\Delta_2)t_{22}\}\left(1-\sqrt{1-(b)}\right)\sqrt{1-\rho^2},\quad \rho\leqslant 1, \tag{23}$$

$$\sigma_{zz}(\rho,0)=-\frac{2p_0}{\pi c}\left(1-\sqrt{1-(a/c)^2}\right)\left(\sin^{-1}(1/\rho)-\frac{1}{\sqrt{\rho^2-1}}\right),\quad \rho\geqslant 1, \tag{24}$$

$$D_z(\rho,0)=-\frac{2q_0}{\pi c}\left(1-\sqrt{1-(b/c)^2}\right)\left(\sin^{-1}(1/\rho)-\frac{1}{\sqrt{\rho^2-1}}\right),\quad \rho\geqslant 1. \tag{25}$$

Eq. (25) is consistent with those obtained by Sosa and Pak (1990) and Park and Sun (1995a,b).

The solution for a point force P_0 and a uniform charge q_0 over the entire crack surface can be obtained from Eqs. (22)–(25) by using the limiting procedure, i.e., $\lim_{a\to 0} p_0\pi a^2=P_0$. For example, the solution for crack surface displacement is

$$w(r,0)=\frac{P_0}{\pi^2 c}\{(\beta_1+\beta_3\Delta_1)t_{11}+(\beta_2+\beta_3\Delta_2)t_{21}\}\sqrt{1-(r/c)^2}$$
$$+\frac{2q_0c}{\pi}\{(\beta_1+\beta_3\Delta_1)t_{12}+(\beta_2+\beta_3\Delta_2)t_{22}\}\sqrt{1-(r/c)^2}. \tag{26}$$

The stress and electric fields near the crack tip are of interest and can be derived from the solution given by Eqs. (22)–(25). Let the origin of a local coordinate R be located at the crack front as shown in Fig. 2. Then,

$$R=r-c=\rho c-c. \tag{27}$$

The near tip fields can be obtained using the standard procedure. For a point force and a point charge, the near tip singular stress and electric displacement are obtained as

$$\sigma_{zz}(R,0)=\frac{P_0}{\pi^2c^2}\sqrt{\frac{\pi c}{2\pi R}},$$
$$D_z(R,0)=\frac{Q_0}{\pi^2c^2}\sqrt{\frac{\pi c}{2\pi R}}. \tag{28}$$

Using the conventional definitions, i.e.,

$$K_{\mathrm{I}}=\lim_{R\to 0}\sqrt{2\pi R}\,\sigma_{zz}(R,0),$$
$$K_{\mathrm{D}}=\lim_{R\to 0}\sqrt{2\pi R}\,D_z(R,0), \tag{29}$$

the stress and electric displacement intensity factors are obtained as

$$K_{\mathrm{I}}=2p_0\sqrt{\frac{c}{\pi}},\quad K_{\mathrm{D}}=2q_0\sqrt{\frac{c}{\pi}},\quad \text{for uniform } p_0 \text{ and } q_0, \tag{30}$$

and

$$K_{\mathrm{I}} = \frac{P_0}{(\pi c)^{3/2}}, \quad K_{\mathrm{D}} = \frac{Q_0}{(\pi c)^{3/2}}, \quad \text{for a point force and charge.} \tag{31}$$

It is noted that K_{I} depends only on the mechanical load, while K_{D} depends only on the electric load.

4. Semicircular surface crack

The crack induced by Vickers indentation (Fig. 3) is modeled as a semicircular surface crack in a half-space as shown in Fig. 4. The only difference between this problem and the penny-shaped crack problem discussed in the previous section is the additional traction free boundary condition on the free surface (the x–z plane, Fig. 4). For homogeneous isotropic elastic solids, the stress intensity factor K_{I} for the semi-circular surface crack is given by Cherepanov (1979) as

$$K_{\mathrm{I}} = \kappa(\theta) K_{\mathrm{I}}^{*}, \tag{32}$$

where

$$\kappa(\theta) = 1 + 0.2\left(\frac{\pi - 2\theta}{\pi}\right)^2, \tag{33}$$

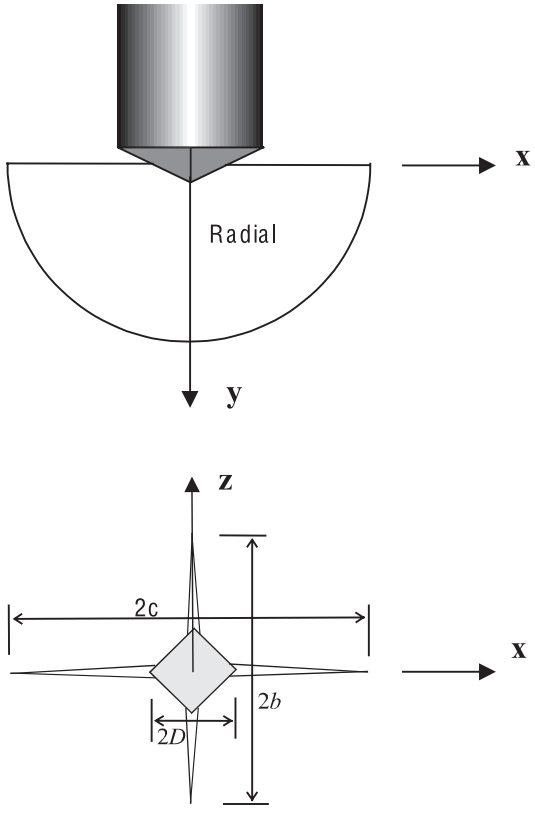

Fig. 3. Dimensions of crack formed by a Vickers indenter.

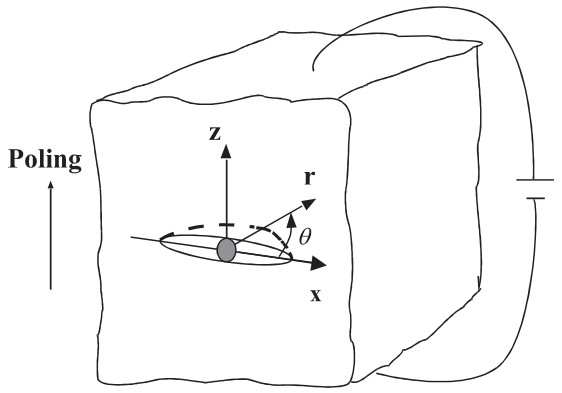

Fig. 4. Illustration of wedge effect due to indentation.

and K_{I}^{*} is the stress intensity factor for the infinite medium with a penny-shaped crack. It is noted that the stress intensity factor varies along the crack front of the semicircular surface crack and assumes the maximum value of $1.2K_{\mathrm{I}}^{*}$ at the free surface, i.e., $\theta = 0,\ \pi$.

Since most piezoceramics are transversely isotropic and the crack surface normal to the z-axis is assumed to be the isotropic plane, we adopt the same correction factor $\kappa(\theta)$ given by Eq. (33) to derive the stress intensity factor for the present problem. Thus, for a point force, P_0 applied in the z-direction at $x = y = z = 0$ in the semicircular surface crack, the stress intensity factor is

$$K_{\mathrm{I}} = \kappa(\theta)\frac{2P_0}{(\pi c)^{3/2}}. \tag{34}$$

Note that the point force for the corresponding penny-shaped crack problem is $2P_0$, used in Eq. (34). In the problem of the penny-shaped crack, the electric displacement D_θ is zero everywhere. Thus, the electric boundary condition at the free surface of the half space problem is satisfied by the penny-shaped crack solution for electric displacement. In view of this, there is no need to correct the electric displacement intensity factor. Thus, for the semicircular surface crack in a half space of piezoceramics with uniform charge q_0 applied on the crack surface, we have

$$K_{\mathrm{D}} = 2q_0\sqrt{c/\pi}. \tag{35}$$

Using the principle of superposition, the expression given by Eq. (35) is also valid for the problem, where the charge is applied remotely (i.e., at a large distance from the crack). Such a boundary condition can be replaced with an equivalent boundary condition in terms of the applied electric field E_z^{∞}. After the constitutive relations Eq. (3) and Eq. (30) are used, the electric displacement intensity factor can be related to the far electric field as

$$K_{\mathrm{D}} = 2E_z^{\infty}\chi_{\mathrm{E}}\sqrt{c/\pi}, \tag{36}$$

where

$$\chi_{\mathrm{E}} = \varepsilon_{33} + \frac{2e_{31}^2c_{33} - 4e_{31}e_{33}c_{13} + e_{33}^2c_{12} + e_{33}^2c_{11}}{c_{12}c_{33} - 2c_{13}^2 + c_{11}c_{33}}. \tag{37}$$

For PZT-4, $\chi_{\mathrm{E}} = 1.15 \times 10^{-8}\ \mathrm{C\,mV^{-1}}$. The first term represents the dielectric effect, while the second term represents the piezoelectric coupling effects.

5. A wedge model for indentation cracks

For unpoled isotropic and homogeneous materials, explicit formulas for the stress intensity factor of a radial crack produced by a Vickers sharp indenter have been empirically derived by many researchers (Chiang et al., 1982; Yoffe, 1982; Anstis et al., 1981). The stress intensity factor K_I can be expressed in terms of material constants, indentation load P, and induced crack length c, as (Anstis et al., 1981)

$$K_I = 0.016\left(\frac{Y}{H}\right)^{1/2} Pc^{-3/2}, \qquad H = \frac{P\sin(\alpha/2)}{2D^2}, \tag{38}$$

where Y and H represent Young's modulus and hardness, respectively, D is the half diagonal of the indentation pyramid and α is the apex angle of the Vickers diamond indenter, which is normally 136°.

The plastic wedge induced by indentation prevents crack surfaces from closing after removal of the indenter, and, thus, causes tensile residual stresses near the crack tip. This wedge action may be represented by a pair of point forces P_0 situated at the "center" $(x = y = z = 0)$ of the crack. The magnitude of P_0 depends on the indentation force and the electric field.

Since the Vickers indentation formula given by Eq. (38) relates the stress intensity factor K_I and the crack length c that is observed on the free surface of the half space, the stress intensity factor K_I should be interpreted as the value at $\theta = 0(\text{or } \pi)$. This formula is assumed to be valid in the absence of electric fields. Thus, for a given indentation force P, we assume that the point force P_0^o gives the same stress intensity factor as the indentation force. From Eqs. (34) and (38), the stress intensity factor induced by a point force P_0^o applied at the "center" of the crack is given by Eq. (34). A wedging force P_0^o is equivalent to P if the corresponding K_I's are equal. As a result, we have

$$0.016\left(\frac{Y}{H}\right)^{1/2} Pc_0^{-1.5} = \kappa_0 \frac{P_0^o}{(\pi c_0)^{3/2}}, \tag{39}$$

where c_0 is the indentation induced crack length in the absence of electric fields, and $\kappa_0 = \kappa(\theta = 0) = 1.2$. From Eq. (39), the equivalent wedging force in the absence of electric fields is established as

$$P_0^o = \frac{0.089}{\kappa_0}\left(\frac{Y}{H}\right)^{1/2} P. \tag{40}$$

It is assumed that the wedge is piezoelectric. For simplicity, we assume that the inelastic region can be represented by a one-dimensional piezoelectric rod element. If a positive electric field is applied, the representative piezoelectric rod would elongate, and wedging force develops. In contrast, if a high negative field is applied to the rod, 180° domain switching would take place since voltage on the crack surface is very high and the length of the rod is very small.

It is not easy to predict when and how completely domain switching would occur in the wedge. A simple empirical model is derived based on the following observations and assumptions:

(1) It is assumed that the domain switching for material in the wedge region under the indenter occurs when negative electric fields are applied. The assumption is made based on the observation that the electric field across the crack surfaces near the crack tip exceed the coercive field.

(2) Based on the experimental observation (Lynch, 1996; Schaufele and Hardtl, 1996), it is assumed that the magnitude of piezoelectric constant d_{33} after domain switching could reduce since 180° domain switching might not be fully completed.

(3) It is observed that under higher compressive stresses, the 180° domain switching could occur more easily (Lynch, 1996). It is expected that the higher indentation load produces a greater compressive stress in the rod (wedge). Based on limited experimental results, it is observed that piezoelectric constants after domain switching may vary with different states of stress. As a result, the greater the indentation load, the smaller the reduction in the piezoelectric constant.

In light of the above observations and assumptions, the piezoelectric constant modified by a reduction factor, $\alpha_{\text{piezo}} d_{33}$, $|\alpha_{\text{piezo}}| \leqslant 1$, is adopted.

Using the crack surface displacement and electric potential given by Eqs. (22) and (23) for the penny-shaped crack problem together with the correction factor κ_0, the crack surface displacement and electric potential at the "center" of the semicircular surface crack is obtained as

$$w(0,0) = \frac{2\kappa_0 P_0}{\pi^2 c}\{(\beta_1 + \beta_3\Delta_1)t_{11} + (\beta_2 + \beta_3\Delta_2)t_{21}\} + \frac{2q_0 c}{\pi}\{(\beta_1 + \beta_3\Delta_1)t_{12} + (\beta_2 + \beta_3\Delta_2)t_{22}\}, \tag{41}$$

and

$$\phi(0,0) = \frac{2\kappa_0 P_0}{\pi^2 c}\{(\gamma_1 + \gamma_3\Delta_1)t_{11} + (\gamma_2 + \gamma_3\Delta_2)t_{21}\} + \frac{2q_0 c}{\pi}\{(\gamma_1 + \gamma_3\Delta_1)t_{12} + (\gamma_2 + \gamma_3\Delta_2)t_{22}\}, \tag{42}$$

respectively, where P_0 is the equivalent point wedging force applied at the "center" of the semicircular crack. Elongation of the rod due to an electric field applied to the rod is

$$\Delta L = -\alpha_{\text{piezo}} d_{33} \Delta\phi, \tag{43}$$

where d_{33} is the original piezoelectric constant, α_{piezo} is the reduction factor associated with the material property change, and $\Delta\phi$ is the electric potential difference given by Eq. (42). It is noted that the contribution to $\Delta\phi$ from wedging force is smaller than that from the applied charge, and, as an approximation, only the second term in Eq. (42) is retained. Meanwhile, deformation in the rod due to an applied charge is secondary and neglected. As a result, the change of crack opening displacement due to electric field is equal to elongation of the rod that is produced by the electric field.

$$w(0,0)|_{P_0=P_0, q_0=q_0, c=c} - w(0,0)|_{P_0=P_0^{\text{o}}, q_0=0, c=c_0} = \Delta L. \tag{44}$$

Substituting Eqs. (41) and (43) into the above equation and solving for P_0, we have

$$P_0 = P_0^{\text{o}}\left(\frac{c}{c_0}\right) - \alpha_{\text{piezo}} k_{\text{D}} c^2 q_0, \tag{45}$$

where

$$k_{\text{D}} = \frac{\pi\{(\gamma_1 + \gamma_3\Delta_1)t_{12} + (\gamma_2 + \gamma_3\Delta_2)t_{22}\}d_{33}}{\kappa_0\{(\beta_1 + \beta_2\Delta_1)t_{11} + (\beta_2 + \beta_3\Delta_2)t_{21}\}}. \tag{46}$$

In Eq. (45), the applied crack surface charge q_0 can also be interpreted as a remotely applied charge that can be represented by an applied electric field E_z. In terms of the applied electric field E_z, we can rewrite Eq. (45) as

$$P_0 = P_0^{\text{o}}\left(\frac{c}{c_0}\right) - \alpha_{\text{piezo}} k_{\text{E}} c^2 E_z, \tag{47}$$

where

$$k_{\text{E}} = k_{\text{D}}\chi_{\text{E}}, \tag{48}$$

in which χ_{E} is given by Eq. (37).

Once the wedging force P_0 is determined by using Eq. (47), the stress intensity factor for the semicircular crack is obtained from Eq. (34) as

$$K_{\mathrm{I}} = \frac{2\kappa(\theta)}{(\pi c)^{3/2}}\left(P_0^{\mathrm{o}}\left(\frac{c}{c_0}\right) - \alpha_{\mathrm{piezo}} k_{\mathrm{E}} c^2 E_z\right). \tag{49}$$

For the indentation crack problem, the stress intensity factor K_{I} is for $\theta = 0°$. Thus, $\kappa(0) = 1.2$.

6. Discussion

The mechanical strain energy release rate proposed by Park and Sun (1995b) includes only mechanical energy released as the crack extends. For Mode I loading, the mechanical strain energy release rate can be obtained using Irwin's crack closure method (Irwin, 1962). For PZT-4, we have

$$G_{\mathrm{I}}^{\mathrm{M}} = \tfrac{1}{2}(1.75 \times 10^{-11} K_{\mathrm{I}}^2 + 2.21 \times 10^{-2} K_{\mathrm{I}} K_{\mathrm{D}}) \ (\mathrm{N\,m^{-1}}), \tag{50}$$

where K_{I} is given by Eq. (49) and K_{D} by Eq. (36). Using the crack lengths at $E_z^{\infty} = 0$ obtained from the Vickers indentation tests, Sun and Park (1995) obtained the critical mechanical strain energy release rates $G_{\mathrm{I}}^{\mathrm{M}} =$ 3.68 and 4.63 $\mathrm{Nm^{-1}}$ for indentation loads $P = 9.8$ N and 49 N, respectively. In terms of the critical $G_{\mathrm{I}}^{\mathrm{M}}$ and a given indentation load, the relation between crack length and electric field can be determined iteratively using Eq. (50). The determination of piezoelectric constant reduction factor α_{piezo} still remains a challenging task. One approach is to choose two data points from each positive and negative electric field to determine this parameter.

For positive electric fields, we take $\alpha_{\mathrm{piezo}} = 0$, because it is assumed that there is no domain switching, and the wedge would elongate the same amount as the surrounding piezoelectric medium, and no additional wedging force due to the electrical field would occur.

For the application of negative electric fields, it is assumed that the 180° domain switching would occur in the wedge, and elongation of the wedge would thus result. It has been observed experimentally (Lynch, 1996) that stress could greatly affect domain switching. As a result, different reduction factors associated with indentation loads 9.8 and 49 N were selected to reflect the fact that greater indentation loads would

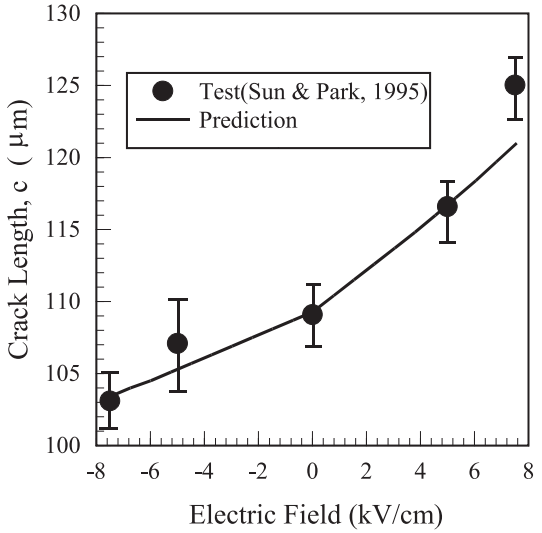

Fig. 5. Prediction of crack length for $P = 9.8$ N.

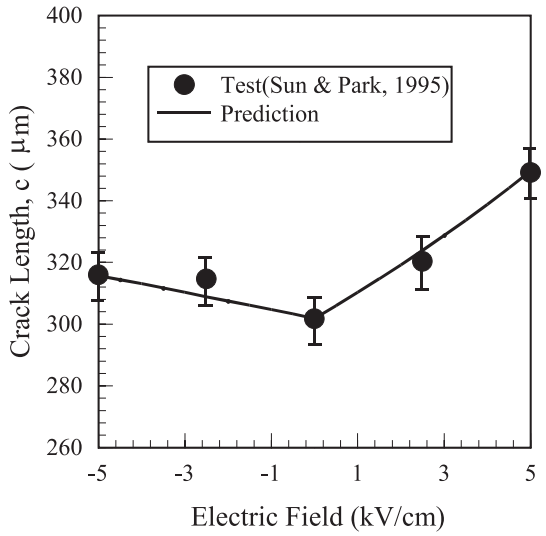

Fig. 6. Prediction of crack length for $P = 49$ N.

produce a higher degree of completion of domain switching. Using the aforementioned approach, we obtain $\alpha_{piezo} = -0.2$ and -0.8 for indentation forces $P = 9.8$ and 49 N, respectively. The negative sign indicates the effect of 180° domain switching. Using these factors, the comparisons between simulation and the experimental results are plotted in Figs. 5 and 6.

Finally, it is noted that a positive electric field through coupling with the tensile residual stress at the crack front would produce a higher driving force G_I^M that would produce a greater crack growth. In contrast, when a negative electric field is applied, due to the wedging effect, tensile stresses at the crack front increase and the crack would still grow to a certain amount.

7. Conclusion

An analytical solution for a penny-shaped crack in an infinite piezoelectric body was derived using Hankel integral transform, from which an approximate solution for indentation cracks was obtained. The concept of a plastic wedge produced by indentation in conjunction with the mechanical strain energy release rate was found able to interpret the electric field effects on indention crack growth. The significance of the model is its simplicity.

Acknowledgements

This work was supported in part by NSF Grant No. 9730123-EEC to Purdue University.

References

Anstis, G.R., Chantikul, P., Lawn, B.R., Marshall, D.B., 1981. A critical evaluation of indentation techniques for measuring fracture toughness: I Direct measurements. Journal of the American Ceramics Society 64, 539–543.

Busbridge, I.W., 1938. Dual integral equations. In: Proceedings of the London Mathematical Society 44, 115.

Cao, H.C., Evans, A.G., 1995. Electric field-induced fatigue crack growth in piezoelectrics. Journal of the American Ceramics Society 17, 1783–1786.

Chandrasekar, S., Chaudhri, M.M., 1993. Indentation cracking in soda-lime glass and Ni–Zn ferrite under Knoop and conical indenters and residual measurements. Philosophical Magazine A 67 (5), 1187–1218.

Chen, W.Q., Shioya, T., Ding, H.J., 1999. The elasto-electric field for a rigid conical punch on a transversely isotropic piezoelectric half-space. Journal of Applied Mechanics 66 (7), 764–771.

Cherepanov, G.P., 1979. Mechanics of Brittle Fracture. McGraw-Hill, New York.

Chiang, S.S., Marshall, D.B., Evans, A.G., 1982. The response of solids to elastic/plastic indentation 1: Stresses and residual stresses. Journal of Applied Physics 53, 312–317.

Cook, R.F., Pharr, G.M., 1990. Direct observation of indentation cracking in glass and ceramics. Journal of the American Ceramics Society 73 (4), 787–817.

Deeg, W.F.J., 1980. The analysis of dislocation, crack, and inclusion problems in piezoelectric solids. Ph.D. Thesis, Stanford University.

Giannakopoulos, A.E., Suresh, S., 1999. Theory of indentation of piezoelectric materials. Acta Mater 47 (7), 2153–2164.

Huang, J.H., 1997. A fracture criterion of a penny shaped crack in transversely isotropic piezoelectric media. International Journal of Solids and Structures 34 (20), 2631–2644.

Irwin, G.R., 1962. Crack extension force for a part-through crack in a plate. Journal of Applied Mechanics 29, 651–654.

Jiang, L.Z., Sun, C.T., 1999. Crack growth behavior in piezoceramics under cyclic loads. Ferroelectrics 233 (3-4), 211–223.

Kassir, M.K., Sih, G.C., 1968. Three-dimensional stresses around elliptical cracks in transversely isotropic solids. Engineering Fracture Mechanics 1, 327–345.

Kogan, L., Hui, C.Y., Molkov, V., 1996. Stress and induction field of a spheroidal inclusion or a penny-shaped crack in a transversely isotropic piezoelectric material. International Journal of Solids and Structures 33 (19), 2719–2737.

Lee, J.S., Jiang, L.Z., 1994. Axisymmetric analysis of multi-layered transversely isotropic elastic media with general innerlayer and support conditions. Stuctural Engineering Mechanics 2 (1), 49–62.

Lynch, C.S., 1996. The effect of uniaxial stress on the electro-mechanical response of 8/65/35 PLZT. Acta Mater 44 (10), 4137–4148.

McMeeking, R.M., 1990. A J-integral for the analysis of electrically induced mechanical stress at cracks in elastic dielectrics. International Journal of Engineering Sciences 28 (7), 607–613.

Okazaki, K., 1984. Mechanical behavior of ferroelectric ceramics. Ceramic Bulletin 63 (9), 1150–1157.

Pak, Y.E., 1990. Crack extension force in a piezoelectric material. Journal of Applied Mechanics 57, 647–653.

Pak, Y.E., 1992. Linear electro-elastic fracture mechanics of piezoelectric materials. International Journal of Fracture 54, 79–100.

Park, S.B., Sun, C.T., 1995a. Effect of electric field on fracture of piezoelectric ceramics. International Journal of Fracture 70, 203–216.

Park, S.B., Sun, C.T., 1995b. Fracture criteria for piezoelectric ceramics. Journal of the American Ceramics Society 78, 1475–1480.

Ramamurty, U., Sridhar, S., Giannakopoulos, A.E., Suresh, S., 1999. An experimental study of spherical indentation on piezoelectric materials. Acta Mater 47 (8), 2417–2430.

Schaufele, A.B., Hardtl, K.H., 1996. Ferroelastic properties of lead zirconate titanate ceramics. Journal of the American Ceramics Society 79, 2637–2640.

Shindo, Y., Ozawa, E., Nowacki, J.P., 1990. Singular stress and electric fields of a cracked piezoelectric strip. Applied Electromagnetics in Material 1, 77–87.

Smith, F.W., Kobayashi, A.S., Emery, A.F., 1967a. Stress intensity factors for penny-shaped cracks, part-1 infinite solid. Journal of Applied Mechanics 34, 947–952.

Smith, F.W., Emery, A.F., Kobayashi A.S, 1967b. Stress intensity factors for penny-shaped cracks, part-2 semi-infinite solid. Transactions of the ASME, Journal of Applied Mechanics 34, 953–959.

Sneddon, I.N., Lowengrub, M., 1968. Crack Problem in the Classical Theory of Elasticity. Wiley, New York.

Sosa, H.A., Pak, Y.E., 1990. Three dimensional eigenfunction analysis of a crack in a piezoelectric material. International Journal of Solids and Structures 26 (1), 1–15.

Sosa, H.A., 1992. On the fracture mechanics of piezoelectric solids. International Journal of Solids and Structures 29, 2613–2622.

Sridhar, S., Giannakopoulos, A.E., Suresh, S., Ramamurty, U., 1999. Electrical response during indentation of piezoelectric materials: A new method for material characterization. Journal of Applied Physics 85 (1), 380–387.

Sun, C.T., Park, S.B., 1995. Determination of fracture toughness of piezoceramics under the influence of electric field using Vickers indentation. In: Proceedings of the 1995 North American Conference on Smart Structures and Materials, 26 February–3 March, San Diego, CA.

Suo, Z., Kuo, C.M., Barnett, D.M., Willis, J.R., 1992. Fracture mechanics for piezoelectric ceramics. Journal of Mechanics and Physical Solids 40 (4), 739–765.

Tiersten, H.F., 1969. Linear Piezoelectric Plate Vibration. Plenum Press, New York.

Titchmarsh, E.C., 1937. Introduction to the Theory of Fourier Integrals. Clarendon Press, Oxford.

Tobin, A.G., Pak, Y.E., 1993. Effect of electric fields on fracture behavior of PZT ceramics. In: Proceedings of the SPIE, Smart Structures and Materials 1916, 78–86.

Tsai, Y.M., 1984. Indentation of a penny-shaped crack by an oblate spheroidal rigid inclusion in a transversely isotropic medium. Journal of Applied Mechanics 51, 811–815.

Wang, B., 1992. Three-dimensional analysis of a flat elliptical crack in a piezoelectric material. International Journal of Engineering Science 30 (6), 781–791.

Wang, Z.K., Huang, S.H., 1995. Fields near elliptical crack tip in piezoelectric ceramics. Engineering Fracture Mechanics. 51 (3), 447–456.

Yoffe, E.H., 1982. Elastic stress fields caused by indenting brittle materials. Philosophical Magazine A 46, 617–628.